

Inhibition of restenosis by tissue factor pathway inhibitor: in vivo and in vitro evidence for suppressed monocyte chemoattraction and reduced gelatinolytic activity

Christoph W. Kopp, Thomas Hölzenbein, Sabine Steiner, Rodrig Marculescu, Helga Bergmeister, Daniela Seidinger, Isabella Mosberger, Christoph Kaun, Manfred Cejna, Reinhard Horvat, Johann Wojta, Gerald Maurer, Bernd R. Binder, Johannes M. Breuss, Rupert C. Ecker, Rainer de Martin, and Erich Minar

Activation of inflammatory and procoagulant mechanisms is thought to contribute significantly to the initiation of restenosis, a common complication after balloon angioplasty of obstructed arteries. During this process, expression of tissue factor (TF) represents one of the major physiologic triggers of coagulation that results in thrombus formation and the generation of additional signals leading to vascular smooth muscle cell (VSMC) proliferation and migration. In this study, we have investigated the mechanisms by which inhibition of coagulation at an early

stage through overexpression of tissue factor pathway inhibitor (TFPI), an endogenous inhibitor of TF, might reduce restenosis. In a rabbit femoral artery model, percutaneous delivery of TFPI using a recombinant adenoviral vector resulted in a significant reduction of the intima-media ratio 21 days after injury. Investigating several markers of inflammation and coagulation, we found reduced neointimal expression of monocyte chemoattractant protein-1 (MCP-1), lesional monocyte infiltration, and expression of vascular TF, matrix metalloproteinase-2 (MMP-2),

and MMP-9. Moreover, overexpression of TFPI suppressed the autocrine release of platelet-derived growth factor BB (PDGF-BB), MCP-1, and MMP-2 in response to factors VIIa and Xa from VSMCs in vitro and inhibited monocyte TF activity. These results suggest that TFPI exerts its action in vivo through not only thrombotic, but also nonthrombotic mechanisms. (*Blood*. 2004;103:1653-1661)

© 2004 by The American Society of Hematology

Introduction

Vascular restenosis after percutaneous balloon angioplasty of atherosclerotic arteries is primarily mediated by intimal hyperplasia due to proliferation of vascular smooth muscle cells (VSMCs)¹ and shrinkage of the vessel wall due to adventitial scarring.² Inflammation and activation of the coagulation cascade are thought to be the key mechanisms triggering this response.

Tissue factor (TF), the major physiologic activator of coagulation in vivo,³ was shown to mediate a prolonged prothrombotic state after balloon angioplasty⁴ by generating active serine proteases of the coagulation cascade, including factor VIIa (VIIa), factor Xa (Xa), and thrombin. Next to their pivotal enzyme function in coagulation these proteases contribute to restenosis by nonthrombotic mechanisms exerting mitogenic and chemotactic effects on VSMCs⁵ and by eliciting a proinflammatory response.⁶ To which extent the TF pathway is involved in the recruitment of monocytes and in vascular matrix degradation after balloon injury is not known.

Tissue factor pathway inhibitor (TFPI), a Kunitz-type protease inhibitor, exerts feedback inhibition on the TF/VIIa-complex in a Xa-dependent manner,⁷ and the coexpression of TFPI and TF was

shown to balance TF activity of injured atherosclerotic plaques.⁸ Furthermore, a direct antiproliferative effect and reduced chemokinesis of VSMCs was reported with overexpression of TFPI in vitro.^{9,10}

In this study, we examined whether catheter-based adenoviral overexpression of TFPI has the potential to limit the proinflammatory, nonthrombotic effects of the activated TF pathway, such as lesional monocyte recruitment and the expression of matrix metalloproteinase-2 (MMP-2) and MMP-9 in an atherosclerotic rabbit injury model for postangioplasty restenosis. Furthermore, the selective activation and inhibition of factor VIIa- and factor Xa-mediated induction of monocyte chemoattractant protein 1 (MCP-1) was studied in control- and TFPI-transfected VSMCs in vitro.

Materials and methods

Cloning of myc-tagged TFPI

In order to differentiate exogenous from endogenous TFPI, a TFPI transgene was generated by polymerase chain reaction (PCR) from

From the 2nd Department of Medicine, Division of Angiology and Cardiology, the Departments of Vascular Surgery, Laboratory Medicine, Biomedical Research, Angiography and Interventional Radiology, Pathology, and Vascular Biology and Thrombosis Research, University of Vienna Medical School, Vienna, Austria; and the Competence Center Bio Molecular Therapeutics, Vienna, Austria.

Submitted April 14, 2003; accepted October 16, 2003. Prepublished online as *Blood* First Edition Paper, October 30, 2003; DOI 10.1182/blood-2003-04-1148.

Supported by the Österreichische National Bank (Jubiläumsfonds Projekt Nr. 8256) and the Hans & Blanca Moser Foundation.

R.C.E. is a developer of software used in this study. He is currently a co-founder and co-owner of TissueGnostics GmbH.

Reprints: Christoph W. Kopp, 2nd Department of Medicine, Division of Angiology, University of Vienna Medical School, Währinger Gürtel 18-20, A-1090 Vienna, Austria; e-mail: christoph.kopp@univie.ac.at.

The publication costs of this article were defrayed in part by page charge payment. Therefore, and solely to indicate this fact, this article is hereby marked "advertisement" in accordance with 18 U.S.C. section 1734.

© 2004 by The American Society of Hematology

full-length human TFPI-cDNA carrying a carboxyterminal myc-tag that codes for a 13-amino acid epitope that is detectable by the monoclonal antibody (mAb) 9E10 (catalog no. OP10, Oncogene; Merck, Darmstadt, Germany). The 1097-bp product including a 5-prime KOZAK sequence was amplified using 5'-GAATTCC ACCATGATTACACA ATGAA-GAAAGTAC-3' as forward (fwd) primer and 5'-AAGCTT TCACCGCAG-CAGATCTTCTTCAGAAATAAGTTTTGTCCATATTTTAAACAA AAATTC-3' as reverse (rev) primer.

Adenoviral vector constructs

The myc-TFPI cDNA or the *lacZ* control transgene (*Ad5lacZ*)¹¹ was cloned into the adenoviral transfer vector pACCMVpLpASR+,¹² and recombinant virus was generated by recombination in 293 cells with the vector pJM17 as described.¹³ Purification of adenovirus preparations was done by 2 consecutive cesium chloride centrifugations.

Cell culture

Rabbit VSMCs (rVSMCs) and human vascular smooth muscle cells (hVSMCs) were cultured by explantation technique from rabbit aortic and human coronary artery segments, respectively. Human umbilical vein endothelial cells (HUVECs) and U937 cells, a human monoblastic cell line (no. CRL-1593.2; American Type Culture Collection [ATCC], Manassas, VA), were cultured by standard technique.

Transfection of rabbit VSMCs in vitro

Ad5TFPI or Ad5*lacZ* adenovirus was diluted to 1×10^9 plaque forming units (pfu)/mL and incubated on 60% confluent VSMCs (15-30 minutes, 37°C, 5% CO₂ in air) under microscopic control. Transgene expression was allowed for 48 hours before in vitro experiments were performed to test the inhibitory capacity of TFPI on coagulation factors.

Immunoprecipitation

Cellular extracts and conditioned supernatant fluid from ³⁵S-labeled VSMCs were immunoprecipitated as described using 5 μg of either antihuman TFPI polyclonal Ab (pAb, no. 4901; American Diagnostica [AD], Greenwich, CT), antihuman c-myc mAb (clone 9E10; Santa Cruz Biotechnology, Santa Cruz, CA) or the control antirabbit pAb (no. 15006; Sigma, St Louis, MO), and antitrinitrophenol mAb (catalog no. 03001D; Pharmingen, San Diego, CA).¹⁴ Denatured samples were separated by 12% sodium dodecyl sulfate-polyacrylamide gel electrophoresis (SDS-PAGE), followed by protein fixation, blotting onto filter paper, and exposure to film.

Inhibition of TF/VIIa and Xa activity by TFPI-transfected VSMCs

Cell-associated and secreted inhibitory activity of TFPI-transfected VSMCs were measured by 1-stage and 2-stage chromogenic assay as described.¹⁵ In brief, serial dilutions of relipidated TF/factor VIIa complex (0-7 pM/7 nM) or factor Xa (0-10 nM) were incubated in 100 μL assay buffer with either transfected or untransfected VSMCs in 96-well plates for 20 minutes at 37°C. After addition of EDTA (ethylenediaminetetraacetic acid)-containing stop buffer, residual amidolytic activity of factor Xa was determined with Spectrozyme Xa (0.5 mM) at A_{405nm} using a kinetic plate reader (DIAS; Dynatech, Chantilly, VA). A standard curve was created with serial dilutions of TF/VIIa complex or factor Xa on plastic. Revelation software (Dynatech) was used for acquisition and analysis.

Inhibition of monocyte (Mo) TF activity by TFPI-transfected VSMCs

U937 cells were stimulated with lipopolysaccharide (LPS, 10 ng/mL) for 16 hours to induce TF expression. After coculture with transfected and untransfected rabbit VSMCs at ratios of 1:1 to 1:10 for 0.5 hours at 37°C and 5% CO₂ in air, plates were centrifuged and TF-dependent amidolytic activity was determined with purified coagulation factor VIIa (7 nM), factor X (300 nM), and Spectrozyme Xa (0.5 mM). Results were compared with a standard curve generated with serial dilutions of relipidated TF/VIIa complex on plastic.

PDGF-BB, MCP-1, and MMP-2 expression by cultured VSMCs

Factor Xa (10 nM)-, factor VIIa (1 nM)-, and thrombin receptor activator peptide (TRAP: SFLLRNPNPKYEPF; 6 μM)-induced expression of platelet-derived growth factor BB (PDGF-BB; catalog no. DBB00, Quantikine; R&D, Minneapolis, MN) and monocyte chemoattractant protein 1 (MCP-1; catalog no. DCP00 Quantikine, R&D) were assessed in time-course experiments (1, 2, 4, 8, and 16 hours) on 24-hour starved untransfected, Ad5TFPI-transfected, or Ad5*lacZ*-transfected human coronary VSMCs by immunoassay. *Trans* retinoic acid (TRA, 10 μM) was used in selected experiments as a partial inhibitor of PDGF-BB.¹⁶ Factor Xa-induced matrix metalloproteinase-2 (MMP-2; catalog no. QIA63; Oncogene) was analyzed from cellular extracts or conditioned supernatant fluid of VSMCs (2.5×10^5) by immunoassay and by SDS-gelatin zymography as described.¹⁷ Densitometry was performed using National Institutes of Health (NIH) Image software (version 1.62; Rockville, MD). Control experiments using the *Limulus* Amoebocyte lysate assay showed that less than 10 pg/mL LPS was present in preparations of coagulation factors, in accordance with the observation that after heating (100°C, 5 minutes) these factors failed to induce PDGF-BB, MCP-1, or MMP-2 production.

Real-time PCR

To detect specific mRNA expression in untransfected, Ad5TFPI-transfected, and Ad5*lacZ*-transfected vessels, total RNA was prepared from minced vascular segments using TRIzol (Invitrogen, Paisley, Scotland). Primers for human TFPI-myc (fwd: 5'-CAA GAA TGT CTG AGG GCA-3', rev: 5'-CTT TCA CCG CAG CAG A-3'; 174 bp, 55°C annealing temperature [AT]), rabbit glyceraldehyde-3-phosphate dehydrogenase (GAPDH; fwd: 5'-ACG GTG CAC GCC ATC ACT GCC-3', rev: 5'-GCC TGC TTC ACC ACC TTC TTG-3'; 266 bp, 63°C AT), rabbit MMP-2 (fwd: 5'-GAA GGT CAA GTG GTC CGT GT-3', rev: 5'-CCG TAC TTG CCA TCC TTC TC-3', 167 bp, 68°C AT), rabbit MMP-9 (fwd: 5'-GCT GTT GAC ATC CTG GCA CT-3', rev: 5'-CTC TCA CCC CAG AAC AAA CC-3'; 154 bp, 65°C AT), rabbit MCP-1 (fwd: 5'-TTC AGC TCC CAT GTG CTT-3', rev: 5'-CTG GAC CCA CTT CTG CT-3'; 204 bp, 62°C AT), and rabbit TF (fwd: 5'-CCG TAC CTG GAC ACA AAC CT-3', rev: 5'-GGG AAT CAC TGC TTG GAC AC-3'; 279 bp, 65°C AT) were designed using the LightCycler Probe Design Software Version 1.0 (Roche, Basel, Switzerland) and the Primer3 Software (http://www-genome.wi.mit.edu/genome_software/other/primer3.html). The following primers were designed to detect human MCP-1 (fwd: 5'-ACTGAAGCTCGCAC TCTC-3', rev: 5'-CTTGGGTTGTGGAGTGAG-3'; 65°C AT) and human GAPDH mRNA levels (fwd: 5'-ACAGTCCATGCCATC ACTGCC-3', rev: 5'-GCCTGCTTACCACCTTCTTG-3'; 65°C AT) in transfected and untransfected VSMCs by real-time PCR. Real-time PCR was performed using LightCycler-RNA Master SYBR Green I (Roche) according to the manufacturer's instructions. The amplification conditions consisted of an initial incubation at 61°C for 20 minutes, followed by incubation at 95°C for 30 seconds, 50 cycles at 95°C for 1 second, the respective indicated annealing temperature for 10 seconds, 72°C for 10 seconds, a melting step from 45°C to 95°C (increasing 0.1°C per second), and a final cooling to 40°C. Data were analyzed using LightCycler Software Version 3.5 (Roche).

Rabbit atherosclerotic femoral artery injury model

Animal experiments were approved by the state committee for animal research and performed according to its guidelines. Focal atherosclerosis of the femoral artery was induced in 40 (N = 40) male New Zealand White (strain KBL-NZW-BR) rabbits (3.2 ± 0.3 kg) by bilateral air-desiccation injury followed by a 1% cholesterol/6% peanut-oil diet for 28 days as described.¹⁸

Angioplasty and percutaneous gene delivery

At 4 weeks after surgery and hypercholesteremic diet, balloon angioplasty and gene delivery were performed at the surgically demarcated site of the femoral stenosis. Under anesthesia and endotracheal ventilation, a 5-French (5-F) introducer was placed through an arteriotomy in the right common carotid artery and advanced to the aortic arch. After an aortoiliac control angiogram and intra-arterial injection of unfractionated

heparin (150 IU/kg), balloon injury (2.5/40 mm, Opta; Cordis, Vienna, Austria) was induced by 3 inflations to 8 atm for 60 seconds each with 60-second intervals. Then, 3 mL adenoviral vector solution (1×10^9 pfu/mL; Ad5TFPI-c-myc, $n = 18$; Ad5lacZ, $n = 18$) or saline control was applied percutaneously over 35 ± 7 seconds at 4 to 6 atm using an infusion catheter (3/20 mm, CrescendoBC; Cordis) and a 10-mL LeVein inflator with pressure gauge assembly (Boston Scientific, Vienna, Austria). A normal rabbit chow diet was continued after angioplasty. Of the animals, 4 received surgery and angioplasty without gene delivery; 3 animals from each group were analyzed on days 2 and 5 after angioplasty (PTA) and gene therapy.

Sample preparation

For analysis, animals received a follow-up angiogram and were killed on day 2 ($n = 6$), day 5 ($n = 6$), or day 21 ($n = 24$) after gene delivery by lethal injection of potassium in profound analgesedation. The abdominal aorta was ligated and flushed with saline followed by surgical preparation and excision of the iliofemoral arteries. Tissue segments were sliced in 3-mm rings and number-coded to identify their relative location to one another, and consecutive ring segments were alternatingly fixed in 4% formalin followed by paraffin embedding or preserved in cryoprotective agent.

Histochemistry and morphometric analysis

There were 2 blinded observers who selected 3 cross sections per vessel with the greatest extent of intimal hyperplasia for histomorphometric quantification. Lumen area (L; A1), (neo-) intima (I), and lumen area (A2) plus medial area (M; A3), delineated by the internal elastic lamina (IEL) and external elastic lamina (EEL), respectively, were quantified by subtraction ($L = A1$; $I = A2 - A1$; $M = A3 - A2$) on digitalized microscope images (BX60 microscope and C-3030 CAMEDIA; Olympus, Tokyo, Japan) of Elastica van Gieson–stained sections using NIH Image software (version 1.62). The ratio of intima to media area was used as a measure of restenosis.

Immunohistochemistry and immunomorphometric analysis

Immunohistochemistry was performed on paraffin-embedded sections after microwave treatment (600 Watts, 2×6 minutes) in citrate buffer (pH 6.0) to detect Kunitz domain 2 (K2) of human TFPI (1:10, mAb, catalog no. 4904; AD), rabbit TF (1:20, mAb, catalog no. 4511; AD), and rabbit macrophages (1:100, mAb, RAM-11, clone M0633; Dako, Glostrup, Denmark) as described.¹⁹ MAbs against MMP-2 (1:100, mAb-3, catalog no. IM33L; Oncogene) and MMP-9 (1:50, mAb-3, catalog no. IM37L; Oncogene) were incubated in Tris (tris(hydroxymethyl)aminomethane)–bovine serum albumin (BSA) 1% on paraffin-embedded autoclaved sections (20 minutes, 2 bar, 10 mM citrate buffer, pH6). Human c-myc epitope was detected on acetone-pretreated cryosections incubated with mouse antihuman c-myc (1:20, 4°C, o/n, mAb, clone 9E10; catalog no. OP10; Oncogene). MCP-1 was detected on blocked, paraffin-embedded sections after overnight incubation with goat antihuman MCP-1/CC chemokine ligand 2 (1:5, 4°C, pAb, catalog no. AF-279-NA; R&D).

In order to visualize primary antibody binding, we used the following secondary reagents: biotinylated antimouse Ab (Vector-BA2000)/mABC-complex with DAB (3,3'-diamino benzidine tetrahydrochloride dihydrate) for detection of c-myc, with AEC (3-amino-9-ethyl-carbazole) for visualization of TFPI-K2 and TF, and with Vector-Vip for MMP-2 and MMP-9. Biotinylated goat anti-mouse immunoglobulin G (IgG, mSS-link; GM601H)/mSS-SA-HRP (HP604H; Biocare) and biotinylated antigen (1:200, Vector)/mSS-SA-HRP (Biocare) followed by AEC were used to detect rabbit macrophages (RAM11) and MCP-1. Immunomorphometry was quantified using AnalySiS software (SIS SoftImaging Software) with a constant color threshold and is given in percent of positive vessel cross-sectional area (% fract. area).

In situ zymography, confocal microscopy, and image cytometry

Gelatinolytic activity of vascular sections was detected by in situ zymography as previously described.²⁰ In brief, gelatin was conjugated with Texas Red (TR) sulphonyl chloride (Molecular Probes, Eugene, OR) according to the manufacturer's instruction. Poly-L-lysine-coated glass slides were covered with conjugated gelatin-TR for 2 hours at room temperature. Thereaf-

ter, excess gelatin-TR was removed and the coating was fixed with 4% paraformaldehyde. After repeat washings in phosphate buffer solution (PBS), glass slides were dried at 37°C. Frozen vascular sections (5 μ m) were placed and incubated with PBS on gelatin-TR films for 32 hours at 37°C in humidified chambers. After fixation in ethanol, slides were mounted in VectorShield with 4', 6'-diamino-2-phenylindol (DAPI; Vector Laboratories, Burlingame, CA) and viewed using a confocal laser scanning microscope (LSM 510; Zeiss, Jena, Germany). Fluorescence signals of DAPI and Texas Red were recorded successively by using the MultiTrack feature of the LSM 510. The DAPI signal was scanned by ultraviolet excitation, Texas Red by a 543-nm He/Ne laser. The full dynamic range of the photomultiplier tubes (PMTs) was used for accurate image cytometry by setting the instrument's sensitivity in a way that the highest fluorescence signals retained just the maximum gray value in the recorded images. Images were recorded at constant PMT sensitivity and at a magnification of $\times 400$ (lens: Zeiss Plan-Neofluar $\times 40/1.30$). Image cytometry was performed using the analysis software TissueQuest (TissueGnostics, Vienna, Austria) based on a method described previously.²¹ This software identified perinuclear areas based on DAPI nuclear staining. The algorithm used measured fluorescence intensity around each individual nucleus in an area of variable size preset by the user. The maximum perinuclear area was defined as a 20-pixel layer around each nucleus, unless neighboring cells

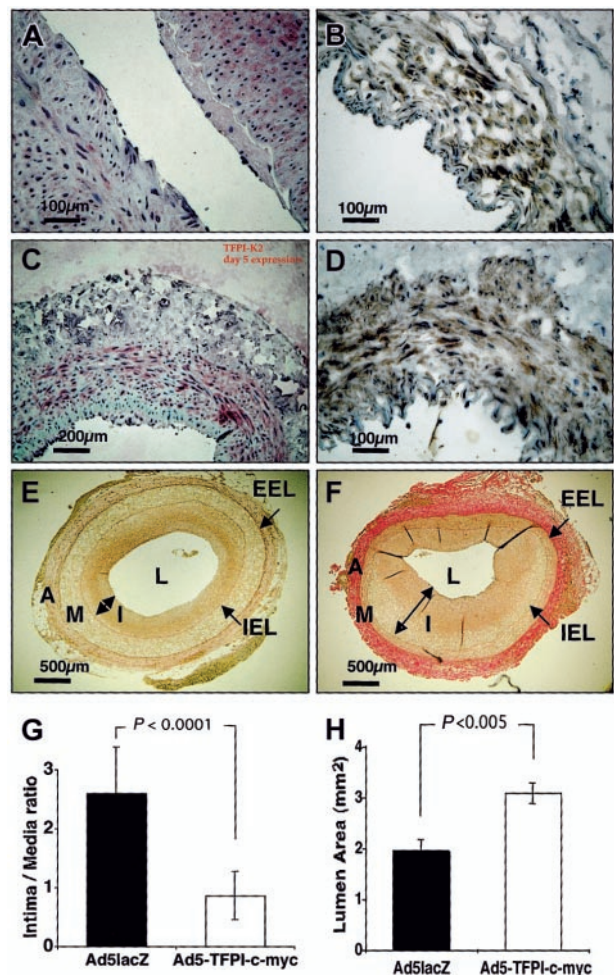


Figure 1. Percutaneous transfection of TFPI inhibits restenosis. Expression of exogenous TFPI detected by immunohistochemistry on days 2 (A-B) and 5 (C-D) after percutaneous transfection with Ad5TFPI-c-myc (1×10^9 pfu/mL) using either the anti-TFPI K2 mAb (A,C) or the anti-c-myc mAb (B,D). Scale bars indicate distance with $\times 20$ (100 μ m) and $\times 10$ (200 μ m) magnification. Intima (I) to media (M) ratio was determined on Elastica van Gieson–stained vascular sections derived from Ad5TFPI-c-myc– (E) and Ad5lacZ-transfected (F) rabbit femoral arteries by histomorphometric analysis. Internal elastic lamina (IEL) and external elastic lamina (EEL) indicated by arrows (\rightarrow) delineate adventitia (A), media (M), and intima (I, \leftrightarrow), which surround the vessel lumen (L). Size bar indicates 500 μ m at $\times 4$ magnification. Results of I/M ratio (G) and residual lumen area (H) are shown as mean \pm SD.

restricted the area of measurement. When integrating the mean relative fluorescence intensity of an individual cell, the software takes into account adjacent cells and ensures that no pixel is measured twice to avoid any overlap with a perinuclear area of a neighboring cell.

Statistics

Morphometric data of femoral arteries in each experimental group are expressed as mean \pm SD unless otherwise stated. The TFPI treatment group and Ad5lacZ control group were compared by 2-sided, unpaired *t* test. Significance was defined as probability less than 5%. Statistical analysis was performed with SPSS software package version 10.0 (SPSS, Chicago, IL) for Macintosh.

Results

Percutaneous overexpression of TFPI and inhibition of restenosis

In order to establish a clinically feasible catheter-based approach, percutaneous unilateral impregnation of Ad5TFPI-c-myc ($n = 18$) or Ad5lacZ ($n = 18$) at a total dose of 3×10^9 pfu was performed in atherosclerotic NZW rabbits using a porous membrane catheter. Percutaneous application of saline to the contralateral femoral artery served as control in all animals. Uniform expression of exogenous myc-tagged TFPI was detected by immunohistochemistry throughout the vascular media using the antihuman TFPI-K2 mAb (Figure 1A,C) and the anti-c-myc mAb (Figure 1B,D) composed of $55\% \pm 12\%$ and $72\% \pm 6\%$ of all media VSMCs on day 2 and day 5 after percutaneous transfection, respectively. Identical results were obtained with antihuman TFPI mAb directed against Kunitz domain 1 (not shown). No cross-reactivity of mAb antihuman TFPI K2 was observed with rabbit TFPI on paraffin-embedded sections. Insignificant expression of exogenous TFPI was detected on day 21 after gene transfer (not shown). No appositional thrombus formation was observed in TFPI-transfected

vessel segments, in contrast to 4 of 18 virus control (Ad5lacZ) and 6 of 40 saline control vessels. In the Ad5lacZ-control group, 2 rabbits had to be killed prematurely (day 2 after angioplasty) because of a stroke; 1 died of septic complications on day 5.

Restenosis as quantitated by intima-media (I/M) ratio was reduced in percutaneously Ad5TFPI-treated arteries (0.9 ± 0.4 I/M; $n = 12$; Figure 1E,G) by $63\% \pm 14\%$ compared with Ad5lacZ virus control (2.7 ± 0.8 I/M, $P < .0001$; Figure 1F-G) 21 days after balloon injury and transfection. Luminal gain was $60 \pm 26\%$ with vascular overexpression of TFPI (3.1 ± 0.8 mm²) compared with Ad5lacZ-transfected control segments (1.9 ± 0.7 mm², $P < .005$; Figure 1H).

Suppression of postangioplasty monocyte recruitment by TFPI

In order to examine the effect of TFPI overexpression on lesional monocyte recruitment after balloon injury, vascular sections were stained for monocyte chemoattractant protein 1 (MCP-1) and infiltrating rabbit monocytes. Both, neointimal MCP-1 expression ($7\% \pm 3\%$ vs $31\% \pm 7\%$; $P = .002$; Figure 2A-B) and lesional monocyte (RAM11⁺ positive) recruitment ($15\% \pm 2\%$ vs $35\% \pm 5\%$; $P = .004$; Figure 2C-D) were significantly suppressed after balloon injury by overexpression of TFPI compared with the virus control. Postinjury increase in vascular MCP-1 mRNA was attenuated in TFPI-treated vessels versus control (Table 1). Monocyte infiltrates in Ad5TFPI-transfected arteries were generally confined to the basal media, supposedly in response to the primary surgical air desiccation injury. In parallel to MCP-1, prolonged TF expression in neointima and media VSMCs was detected in Ad5lacZ-transfected vessel segments until day 21 after angioplasty ($21\% \pm 4\%$ fractional area; Figure 2E) compared with faint TF expression in TFPI-transfected vessels ($11\% \pm 3\%$ fractional area, $P = .037$; Figure 2F), despite strong initial expression of rabbit TF in media VSMCs of both Ad5TFPI- and Ad5lacZ-transfected vessels until day 2 after percutaneous intervention.

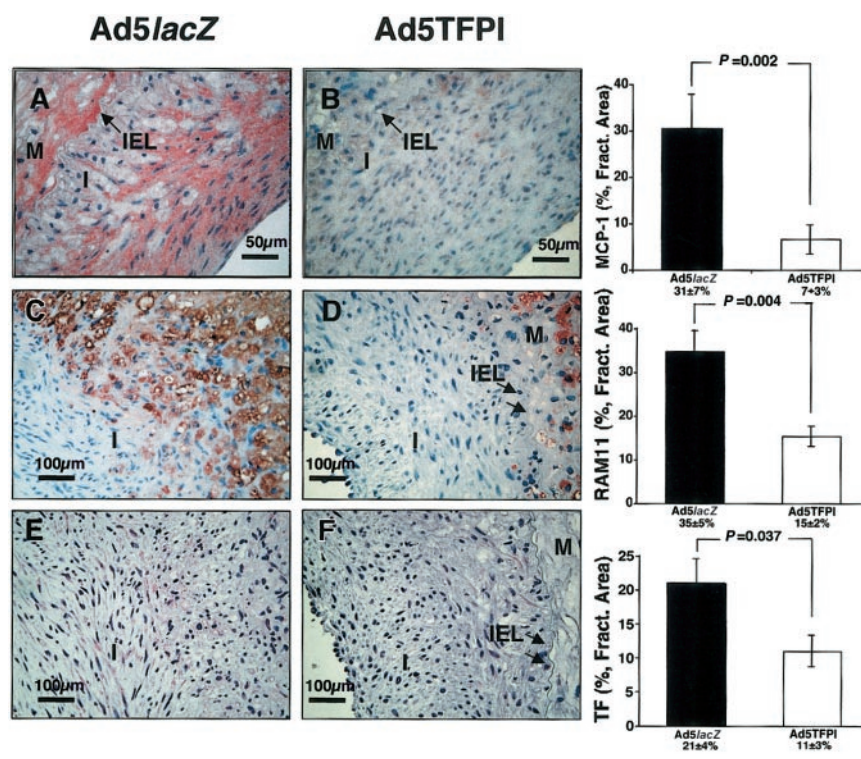


Figure 2. TFPI reduces lesional monocyte recruitment and vascular TF after balloon injury. Immunostaining of MCP-1 (A-B), RAM-11 (C-D), and rabbit TF (E-F) was performed on serial cross sections of Ad5lacZ- and Ad5TFPI-transfected arteries 21 days after balloon injury. Percent fractional area of detected expression is given as mean \pm SEM ($n = 24$) in each group. Arrows (\rightarrow) indicate the internal elastic lamina (IEL) between neointima (I) and media (M).

Table 1. Vascular mRNA with overexpression of TFPI after balloon injury

	TFPI-myc		TF		MCP-1		MMP-2	
	Ad5TFPI	Ad5lacZ	Ad5TFPI	Ad5lacZ	Ad5TFPI	Ad5lacZ	Ad5TFPI	Ad5lacZ
Day 0	0	1	1	1	1	1	1	1
Day 2	1	4.0 ± 2.1	5.1 ± 2.3	5.9 ± 1.2	11.0 ± 2.1	8.8 ± 1.3	5.2 ± 4.0	
Day 5	1.9 ± 0.6	2.2 ± 0.6	3.3 ± 1.1	6.2 ± 1.0	15.7 ± 3.6*	9.4 ± 2.2	14.7 ± 5.0*	
Day 21	0.6 ± 0.2	0.7 ± 0.3	1.9 ± 0.7†	4.2 ± 1.2	17.2 ± 6.2‡	13.7 ± 4.2	32.1 ± 8.2‡	

Values presented as x-fold over baseline ± SEM. T-test Ad5TFPI versus Ad5lacZ: **P* < .05; †*P* < .01; ‡*P* < .001. Human TFPI-myc was not determined in Ad5lacZ-transfected arteries.

Suppression of vascular gelatinolytic activity by TFPI after angioplasty

Next we determined expression of gelatinase mRNA antigen and activity in TFPI- and control virus-transfected balloon-injured vascular segments. MMP-2 expression by VSMCs of the injured media and proliferative neointima was detectable on 57% ± 4% fractional area of Ad5lacZ-transfected vascular cross sections (Figure 3A) compared with 32% ± 6% fractional area of Ad5TFPI-transfected segments (Figure 3B, *P* = .005) on day 21 after angioplasty and gene delivery. At the same time point significantly less MMP-2 mRNA was induced in TFPI-treated vessels compared with control (Table 1).

MMP-9, primarily expressed by infiltrating macrophages, was more abundant in virus control vessel segments (57% ± 6% fractional area; Figure 3C) than in Ad5TFPI-transfected vessels (25.5% ± 5.2% fractional area, *P* < .0001; Figure 3D). Gelatinolytic activity of vascular sections was significantly suppressed in TFPI-transfected (163 ± 44 Texas Red [TR]-Intensity; Figure 3F) compared with virus-control vascular segments (111 ± 37 TR-Intensity; Figure 3E) as detected by in situ zymography (*P* = .017).

Expression of exogenous TFPI in transfected VSMCs

To further examine potential mechanisms of TFPI contributing to the inhibition of restenosis observed in vivo, we conducted a series of in vitro experiments. Immunoprecipitation of cytoplasmic

protein extracts prepared from Ad5TFPI-c-myc-transfected rabbit VSMCs showed a double band at 41 and 43 kDa detectable with both the pAb against human TFPI and the mAb directed against the human c-myc peptide (Figure 4A), confirming synthesis and expression of myc-tagged, full-length human TFPI. No labeled protein was precipitated with the respective polyclonal (Figure 4, lane 6) and monoclonal (lane 8) control antibody. In untreated (Figure 4, lanes 1-2) or Ad5lacZ-transfected rabbit VSMCs (lanes 3-4) no precipitation occurred either with control^{2,4} or with specific pAb for TFPI,^{1,3} excluding cross-reactivity with endogenous rabbit TFPI. As TFPI is a secretory protein, a similar band pattern showing a single band at 43 kDa was precipitated with anti-TFPI and anti-c-myc Ab from supernatant fluid conditioned for 16 hours on ³⁵S-labeled Ad5TFPI-c-myc-transfected VSMCs (Figure 4B).

Direct anticoagulant activity of TFPI-transfected VSMCs

As we found high-level cell-associated expression of TFPI by immunohistochemistry, we next determined the direct anticoagulant activity of Ad5TFPI-transfected VSMCs for purified coagulation factors and monocyte TF activity. Factor Xa generation by relipidated TF/VIIa-complex was reduced by 89% ± 3% (***P* < .001; Figure 4C) and purified factor Xa activity was reduced by 57% ± 14% (***P* < .001; Figure 4D) on Ad5TFPI-transfected rabbit VSMCs compared with untransfected rabbit VSMCs. Monocyte TF activity of LPS-activated U937 cells was

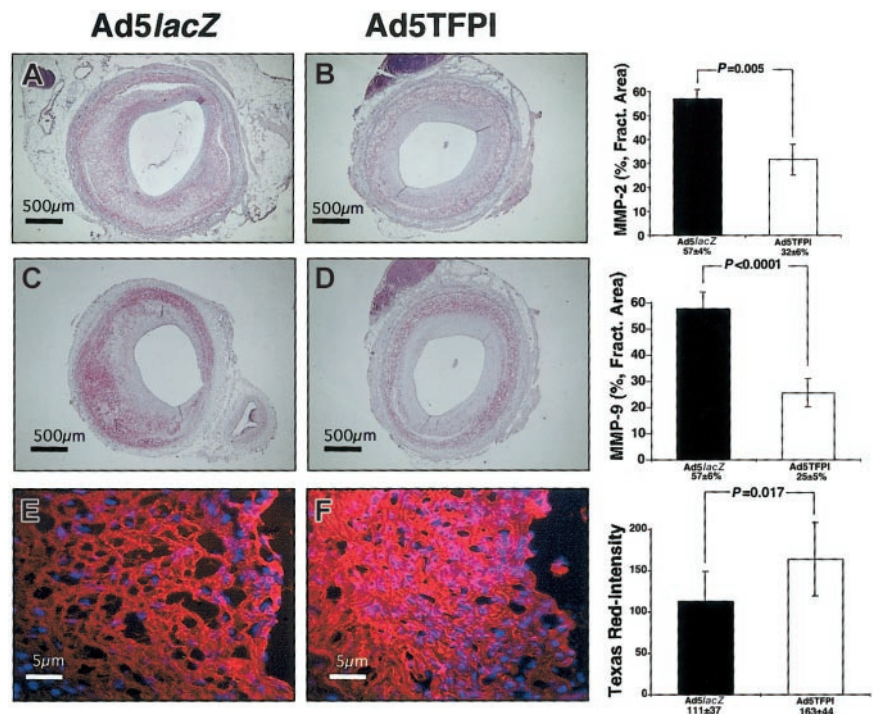


Figure 3. TFPI mediates suppression of vascular gelatinolytic activity after balloon injury. Expression of rabbit MMP-2 (A-B) and rabbit MMP-9 (C-D) in control virus (Ad5lacZ)- and Ad5TFPI-transfected rabbit femoral arteries 21 days after PTA and gene delivery. The size bar indicates 500 μm at × 4 magnification. Percent fractional area is given as mean ± SEM (n = 24) in each group. Gelatinolytic activity of Ad5lacZ-transfected (E) and Ad5TFPI-transfected (F) vessel segments as shown by in situ zymography and quantitated using TissueQuest software. Stains used: Vector VIP Substrate for Peroxidase (A-D); and Texas Red and DAPI (E-F).

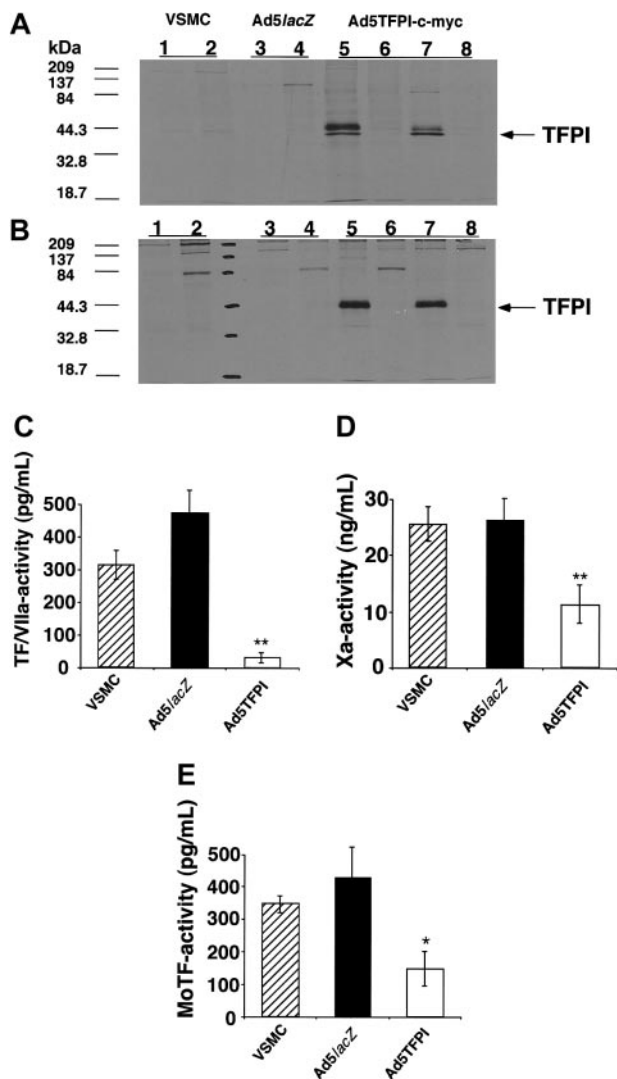


Figure 4. TFPI overexpressed in VSMCs inhibits monocyte TF activity. Immunoprecipitation of cellular extracts (A) or conditioned supernatant fluid (B) from ^{35}S -labeled untreated (VSMC), control virus-transfected (Ad5lacZ), or TFPI-transfected (Ad5TFPI-c-myc) rabbit VSMCs with either control antibody (lanes 2, 4, 6, and 8), antibody specific for human TFPI (lanes 1, 3, and 5), or the c-myc epitope (lane 7). Inhibition of factor Xa activity (C), TF/VIIa-complex activity on factor X (D), and of LPS-induced U937 monocyte TF activity (E) by untreated (▨), Ad5lacZ-transfected (■), and Ad5TFPI-c-myc-transfected (□) rabbit VSMCs determined by chromogenic assay. Data are expressed as mean \pm SD; * $P < .01$, ** $P < .001$.

inhibited by $65\% \pm 12\%$ (* $P = .0046$; Figure 4E) after coculture with TFPI-transfected VSMCs at a 1:1 cell ratio compared with untransfected rabbit VSMCs. In all 3 assay systems, no inhibition was observed with Ad5lacZ-transfected VSMCs. Recalcified clotting time of citrated rabbit plasma was significantly prolonged in the presence of Ad5TFPI-transfected HUVECs (680 ± 102 seconds) compared with Ad5lacZ-transfected HUVECs (533 ± 53 seconds, $P = .018$), and both were significantly prolonged compared with the clotting time on plastic (370 ± 32 seconds, $P < .001$), confirming species compatibility (data not shown).

Inhibition of factor VIIa- and factor Xa-induced PDGF-BB and MCP-1 by TFPI in VSMCs

As neointimal MCP-1 was suppressed by TFPI in vivo, we next examined the potential role of the TF pathway in inducing MCP-1 in VSMCs in vitro. MCP-1 mRNA (Figure 5B, 16-hour time point) and protein of VSMCs were increased in response to factor Xa

(Figure 5C), factor VIIa (Figure 5D), and TRAP (Figure 5E) in a time-dependent fashion. Adenoviral infection of VSMCs using the control virus Ad5lacZ generally impaired MCP-1 induction by these coagulation factors. However, factor Xa-mediated (** $P < .001$) and factor VIIa-mediated ($\#P < .05$), but not TRAP-mediated MCP-1 secretion, were significantly reduced by Ad5TFPI-transfected VSMCs compared with virus control after 16-hour stimulation (Figure 5C-E) in accordance with our in vivo finding. Similarly, induction of MCP-1 mRNA by factors VIIa and Xa but not TRAP was significantly inhibited by Ad5TFPI-transfected VSMCs compared with the Ad5lacZ control (Figure 4B). Since pilot experiments showed that coincubation with retinoic acid—a known suppressor of platelet-derived growth factor (PDGF)-induced transcription¹⁶—antagonized MCP-1 induction by approximately 40% to 50%, we further tested the factor VIIa-, factor Xa-, and TRAP-mediated autocrine PDGF release in untransfected, and TFPI- and control virus-transfected VSMCs. PDGF-BB, a known inducer of MCP-1 in fibroblasts,¹⁶ was significantly increased in media conditioned by factor Xa- (** $P < .001$), factor VIIa- ($\#P = .04$), or TRAP-stimulated ($\#P = .03$) untransfected VSMCs after 16 hours (Figure 5). Overexpression of Ad5TFPI in VSMCs significantly decreased factor Xa-stimulated (** $P < .001$; Figure 5) and lowered factor VIIa-stimulated ($P =$ not significant) autocrine release of PDGF-BB compared with control virus transfection. TRAP-induced PDGF release was not antagonized by overexpression of TFPI compared with virus control.

Inhibition of factor Xa-induced MMP-2 by TFPI in VSMCs

In contrast to vascular MMP-9 expression, which was exclusively associated with macrophages and diminished in TFPI-transfected vessels due to reduced lesional monocyte recruitment, vascular MMP-2 expression was confined to neointimal VSMCs but similarly suppressed in TFPI-transfected vessels. Therefore, we examined factor Xa stimulation of untransfected, and TFPI- and control virus-transfected VSMCs in vitro. Coagulation factor Xa stimulation for 24 hours increased cell-associated and secreted MMP-2 in VSMCs by $34 \pm 3\%$ ($\#P = .01$; Figure 6A) and $45\% \pm 8\%$ ($\#P = .03$; Figure 6B), respectively, and Ad5TFPI transfection of VSMCs significantly inhibited Xa-dependent induction of cell-associated (by $75\% \pm 1\%$, ** $P = .0002$; Figure 6A) and secreted (by $82\% \pm 2\%$, ** $P = .005$; Figure 6B) MMP-2 compared with control. Factor Xa-induced latent MMP-2 activity (Figure 6C, lane 4: 2730 ± 91 units) was reduced by 30% in TFPI-transfected rabbit VSMCs (lane 3: 1914 ± 39 units, $P = .01$) as shown by gelatin zymography (Figure 6C). No latent MMP-2 activity was detected without factor Xa stimulation in Ad5TFPI-transfected (Figure 6C, lane 1) and untransfected (lane 2) rabbit VSMCs.

Discussion

Restenosis caused by local thrombus formation and inflammation in response to balloon injury¹ remains a major limitation in successful endovascular therapy of obstructive atherosclerosis.²² As fibrin- and platelet-rich thrombi were shown to play a key role in neointima formation, thrombosis soon became a target for antirestenotic therapy.²³ Despite an impressive reduction of restenosis with systemically applied inhibitors of the coagulation cascade in experimental animal models,²⁴ the improvement of periprocedural antithrombotic strategies in the clinical setting of angioplasty using combined regimens of anticoagulant and antiplatelet agents did not significantly lower the incidence of restenosis in

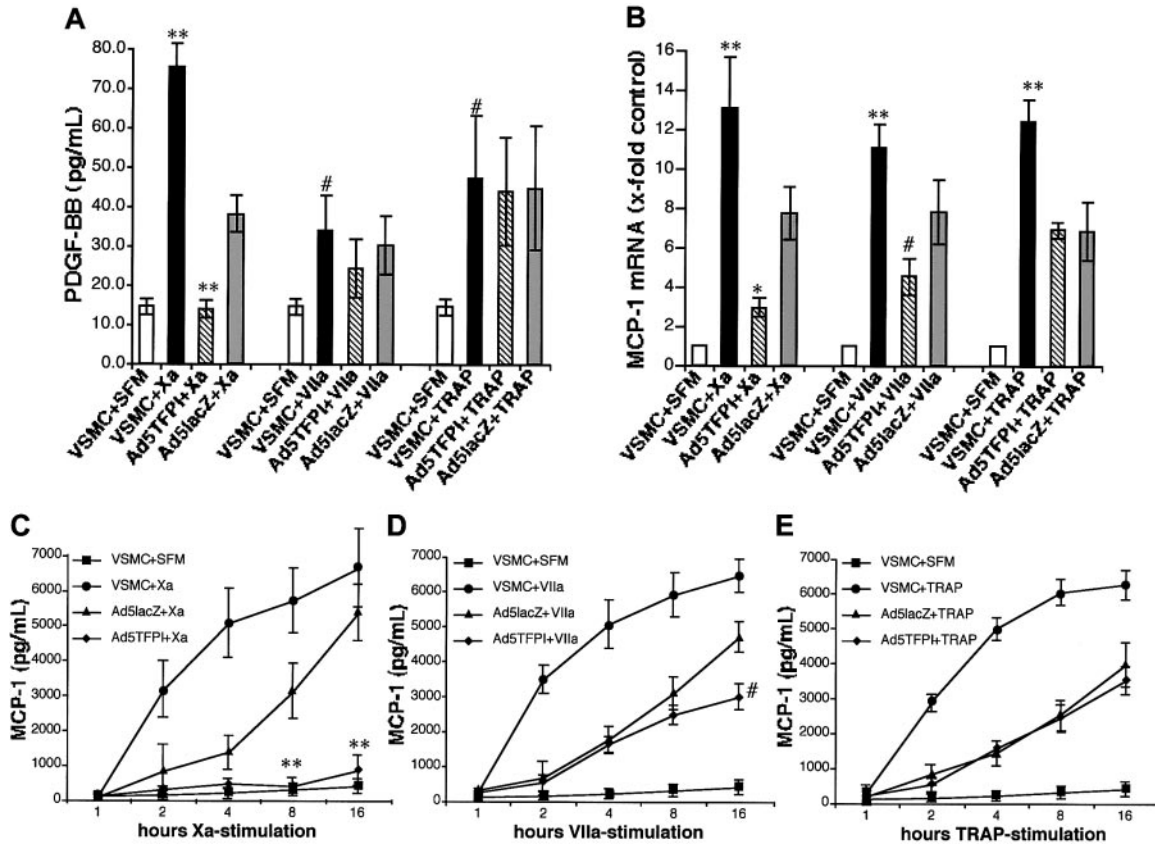


Figure 5. Inhibition of PDGF and MCP-1 induction by TFPI in VSMCs. PDGF (panel A, 16-hour time point) and MCP-1 (C-E, in time course) were determined by immunoassay after stimulation of either untransfected (VSMC), control virus (Ad5lacZ)-transfected, or Ad5TFPI-transfected VSMCs with factor Xa, factor VIIa, or TRAP. Serum-free media (SFM) served as control. MCP-1 mRNA was determined by real-time PCR after 16-hour stimulation (B). Data are mean ± SD of at least 4 experiments. #*P* < .05, **P* < .01, ***P* < .001.

humans.²⁵ The failure of systemically administered antithrombotic therapy to efficiently interfere with clinical postangioplasty restenosis in humans is thought to be a result of insufficient local concentration of antithrombotic drugs at sites of balloon injury. Thus, various studies with local application strategies of TFPI protein^{23,24,26-31} or TFPI gene³²⁻³⁵ were undertaken to antagonize local thrombus formation, intimal hyperplasia, or vascular remodel-

ing, generally using a surgical approach for irrigation or transfection. In contrast to these studies, we sought to locally overexpress TFPI using a clinically feasible, catheter-based approach. Short-term adenoviral transfection with a virus titer below the vector-dependent inflammatory threshold ($< 1.6 \times 10^9$ pfu/mL)³⁶ resulted in transmural expression of the transgene in approximately 60% of media VSMCs. The lack of appositional thrombus formation in TFPI-transfected balloon-injured vessels suggested effective local inhibition of procoagulant TF activity in vivo. Exogenous TFPI was detected at high levels in transfected VSMCs and in media conditioned by these cells in vitro, suggesting paracrine actions of the transgene product.

We further investigated the capacity and mechanisms of TFPI locally secreted into the plaque environment to inhibit restenosis. Importantly, we found a TFPI-dependent reduction in restenosis and identified both anticoagulant and anti-inflammatory mechanisms responsible for this phenomenon. First, we demonstrated that the TFPI-mediated anticoagulant activity in VSMCs was limited not only to the inhibition of purified coagulation factor Xa and TF/VIIa, but also exerted a direct inhibition of monocyte TF, a known determinant of the adhesive and migratory monocyte phenotype.³⁷ Second, our data provided in vitro and in vivo evidence for reduced autologous MCP-1 activity of TFPI-transfected VSMCs. In vitro, coagulation factor Xa- and factor VIIa-induced MCP-1 secretion of VSMCs was significantly reduced by adenoviral overexpression of TFPI compared with virus control. A similar effect was observed for PDGF-BB, which was induced by factors Xa and VIIa stimulation of VSMCs and suppressed by overexpression of TFPI. A functional link between

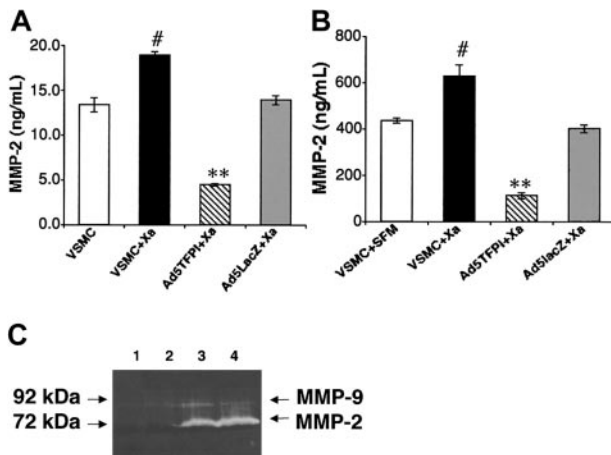


Figure 6. Inhibition of Xa-induced MMP-2 by TFPI in VSMCs. Cell-associated (A) and secreted (B) MMP-2 expression was determined by immunoassay in untreated (□) and factor Xa-stimulated, untransfected (■) VSMCs, and Ad5TFPI-transfected (▨) and Ad5lacZ-transfected (▩) VSMCs. Data are mean ± SEM of 3 experiments. #*P* < .05, ***P* < .001. MMP-2 activity of untransfected (lanes 2 and 4) and TFPI-transfected (lanes 1 and 3) rabbit VSMCs was determined after stimulation with factor Xa (lanes 3-4) by gelatin zymography (C).

PDGF-BB and MCP-1 secretion in VSMCs by coagulation factors of the TF pathway *in vitro* was supported by the suppressed induction of MCP-1 upon coinubation with *trans* retinoic acid, a partial inhibitor of PDGF-BB-mediated transcriptional activity.¹⁶ *In vivo*, vascular overexpression of TFPI diminished neointimal expression of MCP-1, reduced lesional recruitment of monocytes (a known determinant of the extent of restenosis),³⁸ and shortened the expression of vascular TF (previously shown to be directly induced by MCP-1 in aortic smooth muscle cells).³⁹ Third, we demonstrated diminished expression of monocyte-associated MMP-9 after angioplasty of TFPI-transfected atherosclerotic vessels correlating with reduced lesional infiltration of RAM11⁺ macrophages. Together, these mechanisms contributed to a significant reduction in restenosis mediated by overexpression of TFPI.

Decreased matrix degradation in TFPI-transfected balloon-injured vessel segments was further supported by reduced expression of vascular MMP-2 mRNA and antigen *in vivo* and by the suppression of vascular gelatinolytic activity of frozen sections on films of Texas Red-conjugated gelatin *ex vivo*. In addition we could demonstrate diminished Xa-dependent MMP-2 secretion in TFPI-transfected VSMCs *in vitro*. These findings are in accordance with factor Xa-regulated expression of MMP-2 in VSMCs as reported by Rauch et al.⁴⁰ Intimal hyperplasia may thus be orchestrated not only by MCP-1-mediated direct mitogenic activity⁴¹ and its capacity to attract monocytes to balloon injured vessels, but also by monocyte (MMP-9)- and VSMC (MMP-2)-directed extracellular matrix degradation. In contrast to TFPI-2, which was shown to directly antagonize the activity of MMP-1, -2, -9, and -13,⁴² TFPI-1 established its anti-inflammatory function indirectly by reducing factor VIIa- and factor Xa-dependent stimulation of VSMCs.

In our *in vitro* experiments, control virus transfection significantly inhibited Xa-induced MCP-1 and PDGF mRNA expression despite correction for loading using the housekeeping gene GADPH. Similarly, Xa-, VIIa/TF-, and TRAP-induced MCP-1 antigen expression was significantly inhibited by control adenoviral transfection despite correction for protein concentration. One explanation for this phenomenon may relate to the potential of E3-containing first-generation adenoviral vectors—as used in our experimental systems—to attenuate nuclear factor κ B (NF κ B)-dependent gene expression. As shown previously, NF κ B and p90 are required for optimum PDGF induction of MCP-1.⁴³ Adenoviral E3 was shown to prevent NF κ B from entering the nucleus by preventing activation of the I κ B kinase complex, which is responsible for the inhibitor of NF κ B (I κ B) phosphorylation and degradation, and thus retains NF κ B in the cytoplasm in an inactive state.⁴⁴ Concerning the correlation with *in vivo* data, we have previously shown that activation of NF κ B significantly contributes to lumen loss in a rabbit iliac artery balloon angioplasty model.⁴⁵ Thus E3-containing adenoviral overexpression by itself may contribute

to the inhibition of restenosis by interfering with activation and nuclear translocation of NF κ B. Aware of the limitation of the adenoviral-vector system used for gene therapy and despite careful correction for virus background, we observed significant inhibition of Xa-induced PDGF-BB and of Xa- and VIIa-induced MCP-1, but not of TRAP-mediated induction of PDGF or MCP-1. Thus, only proteases directly antagonized by TFPI but not the direct protease-activated receptor-1 (PAR-1) agonist were inhibited by Ad5TFPI-transfected VSMCs, which suggests substrate specificity of the transgene product.

Here, we first demonstrated that overexpression of TFPI in VSMCs regulates factor VIIa- and factor Xa-induced PDGF-BB and MCP-1 *in vitro*. This is in line with previous studies, which reported autocrine release of PDGF, a potent inducer of MCP-1 transcription,¹⁶ in response to factors VIIa⁴⁶ and Xa stimulation^{47,48} in various cell systems. We further showed reduced vascular MCP-1 expression, lesional macrophage accumulation, and intimal hyperplasia in balloon-injured TFPI-transfected arteries *in vivo*. Previous studies reported that selective inhibition of PDGF⁴⁹ or MCP-1⁵⁰ interferes with restenosis and found an *in vivo* relationship between PDGF and MCP-1 in the process of restenosis.⁵¹ In addition, both factors were demonstrated to induce TF activity in peripheral blood monocytes,⁵² which we found effectively antagonized by TFPI-transfected VSMCs. Thus, it is conceivable that TFPI-mediated inhibition of MCP-1-dependent mechanisms such as smooth muscle cell proliferation, monocyte chemoattraction, and TF induction may be central to the antirestenotic effect observed in our study.

The receptors for factor VIIa- and factor Xa-signaling MCP-1 induction on VSMCs remain to be defined. TF and effector-cell protease receptor-1 (EPR-1) are the most likely candidate receptors for factors VIIa⁴⁶ and Xa,⁴⁸ respectively, as—similar to our finding in VSMCs—autocrine PDGF release was demonstrated due to these receptor-ligand interactions in fibroblasts. However, a role of PAR-2 as the potential receptor for both factor VIIa/TF and Xa cannot be excluded.⁵³ This proinflammatory pathway appears to be different from the mitogenic effect of factor Xa on VSMCs, which was reported to be independent of PDGF.⁵⁴

In conclusion, our data emphasize a cross-talk between thrombosis and inflammation, both, on the pro- and anticoagulant level of the TF pathway by showing that TF-dependent coagulation and inflammation orchestrate key mechanisms in the process of restenosis, which can effectively be inhibited by catheter-based, adenoviral overexpression of TFPI.

Acknowledgment

The authors are indebted to Dr Tamara Kopp for thoughtful revision of the manuscript.

References

- Libby P, Schwartz D, Brogi E, Tanaka H, Clinton SK. A cascade model for restenosis: a special case of atherosclerosis progression. *Circulation*. 1992;86(suppl 6):II147-II152.
- Scott NA, Cipolla GD, Ross CE, et al. Identification of a potential role for the adventitia in vascular lesion formation after balloon overstretch injury in porcine coronary arteries. *Circulation*. 1996;93:2178-2187.
- Morrissey JH, Fakhrai H, Edgington TS. Molecular cloning of the cDNA for tissue factor, the cellular receptor for the initiation of the coagulation protease cascade. *Cell*. 1987;50:129-135.
- Marmor JD, Rossikhina M, Guha A, et al. Tissue factor is rapidly induced in arterial smooth muscle after balloon injury. *J Clin Invest*. 1993;91:2253-2259.
- Ko FN, Yang YC, Huang SC, Ou JT. Coagulation factor Xa stimulates platelet-derived growth factor release and mitogenesis in cultured vascular smooth muscle cells of rat. *J Clin Invest*. 1996;98:1493-1501.
- Senden NHM, Jeunhomme TMAA, Heemskerck JWM, et al. Factor Xa induces cytokine production and expression of adhesion molecules by human umbilical vein endothelial cells. *J Immunol*. 1998;161:4318-4324.
- Broze GJ Jr, Girard TJ, Novotny WF. Regulation of coagulation by a multivalent Kunitz-type inhibitor. *Biochemistry*. 1990;29:7539-7546.
- Caplice NM, Mueske CS, Kleppe LS, Simari RD. Presence of tissue factor pathway inhibitor in human atherosclerotic plaques is associated with reduced tissue factor activity. *Circulation*. 1998;98:1051-1057.
- Kamikubo Y, Nakahara Y, Takemoto S, Hamuro T, Miyamoto S, Funatsu A. Human recombinant tissue factor pathway inhibitor prevents the proliferation of cultured human neonatal aortic smooth muscle cells. *FEBS Lett*. 1997;407:116-120.
- Sato Y, Kataoka H, Asada Y, et al. Overexpression of tissue factor pathway inhibitor in aortic

- smooth muscle cells inhibits cell migration induced by tissue factor/factor VIIa complex. *Thromb Res.* 1999;94:401-406.
11. Stratford-Perricaudet LD, Briand P, Perricaudet M. Feasibility of adenovirus-mediated gene transfer in vivo. *Bone Marrow Transplant.* 1992;9:151-152.
 12. Gomez-Foix AM, Coats WS, Baque S, Alam T, Gerard RD, Newgard CB. Adenovirus-mediated transfer of the muscle glycogen phosphorylase gene into hepatocytes confers altered regulation of glycogen metabolism. *J Biol Chem.* 1992;267:25129-25134.
 13. Wrighton CJ, Hofer-Warbinek R, Moll T, Eytner R, Bach FH, de Martin R. Inhibition of endothelial cell activation by adenovirus-mediated expression of I kappa B alpha, an inhibitor of the transcription factor NF-kappa B. *J Exp Med.* 1996;183:1013-1022.
 14. Kopp CW, Robson SC, Siegel JB, et al. Regulation of monocyte tissue factor activity by allogeneic and xenogeneic endothelial cells. *Thromb Haemost.* 1998;79:529-538.
 15. Kopp CW, Siegel JB, Hancock WW, et al. Effect of porcine endothelial tissue factor pathway inhibitor on human coagulation factors. *Transplantation.* 1997;63:749-758.
 16. Ping D, Boekhoudt G, Boss JM. Trans-Retinoic acid blocks platelet-derived growth factor-BB-induced expression of the murine monocyte chemoattractant-1 gene by blocking the assembly of a promoter proximal Sp1 binding site. *J Biol Chem.* 1999;274:31909-31916.
 17. Yaguchi T, Fukuda Y, Ishizaki M, Yamanaka N. Immunohistochemical and gelatin zymography studies for matrix metalloproteinases in bleomycin-induced pulmonary fibrosis. *Pathol Int.* 1998;48:954-963.
 18. Gertz SD, Fallon JT, Gallo R, et al. Hirudin reduces tissue factor expression in neointima after balloon injury in rabbit femoral and porcine coronary arteries. *Circulation.* 1998;98:580-587.
 19. Speiser W, Kapiotis S, Kopp CW, et al. Effect of intradermal tumor necrosis factor-alpha-induced inflammation on coagulation factors in dermal vessel endothelium: an in vivo study of human skin biopsies. *Thromb Haemost.* 2001;85:362-367.
 20. Kunugi S, Fukuda Y, Ishizaki M, Yamanaka N. Role of MMP-2 in alveolar epithelial repair after bleomycin administration in rabbits. *Lab Invest.* 2001;81:1309-1318.
 21. Steiner GE, Ecker RC, Kramer G, Stockenhuber F, Marberger MJ. Automated data acquisition by confocal laser scanning microscopy and image analysis of triple stained immunofluorescent leukocytes in tissue. *J Immunol Methods.* 2000;237:39-50.
 22. Popma JJ, Califf RM, Topol EJ. Clinical trials of restenosis after coronary angioplasty. *Circulation.* 1991;84:1426-1436.
 23. Asada Y, Hara S, Tsuneyoshi A, et al. Fibrin-rich and platelet-rich thrombus formation on neointima: recombinant tissue factor pathway inhibitor prevents fibrin formation and neointimal development following repeated balloon injury of rabbit aorta. *Thromb Haemost.* 1998;80:506-511.
 24. Jang Y, Guzman LA, Lincoff AM, et al. Influence of blockade at specific levels of the coagulation cascade on restenosis in a rabbit atherosclerotic femoral artery injury model. *Circulation.* 1995;92:3041-3050.
 25. Acute platelet inhibition with abciximab does not reduce in-stent restenosis (ERASER study): the ERASER Investigators. *Circulation.* 1999;100:799-806.
 26. Brown DM, Kania NM, Choi ET, et al. Local irrigation with tissue factor pathway inhibitor inhibits intimal hyperplasia induced by arterial interventions. *Arch Surg.* 1996;131:1086-1090.
 27. Han X, Girard TJ, Baum P, Abendschein DR, Broze GJ Jr. Structural requirements for TFPI-mediated inhibition of neointimal thickening after balloon injury in the rat. *Arterioscler Thromb Vasc Biol.* 1999;19:2563-2567.
 28. Roque M, Reis ED, Fuster V, et al. Inhibition of tissue factor reduces thrombus formation and intimal hyperplasia after porcine coronary angioplasty. *J Amer Coll Cardiol.* 2000;36:2303-2310.
 29. Huynh TTT, Davis MG, Thompson MA, Ezekowitz MD, Hagan PO, Annex BH. Local treatment with recombinant tissue factor pathway inhibitor reduces development of intimal hyperplasia in experimental vein grafts. *J Vasc Surg.* 2001;33:400-407.
 30. Sun L-B, Utho J, Moriyama S, Tagami H, Okamoto K, Kitamura N. Topically applied tissue factor pathway inhibitor reduced intimal thickness of small arterial autografts in rabbits. *J Vasc Surg.* 2001;34:151-155.
 31. Nakamura Y, Nakamura K, Ohta K, et al. Anti-inflammatory effect of long-lasting locally-delivered recombinant tissue factor pathway inhibitor after balloon angioplasty. *Basic Res Cardiol.* 2002;97:198-205.
 32. Zoldhelyi P, Chen ZQ, Shelat HS, McNatt JM, Willerson JT. Local gene transfer of tissue factor pathway inhibitor regulates intimal hyperplasia in atherosclerotic arteries. *Proc Natl Acad Sci U S A.* 2001;98:4078-4083.
 33. Singh R, Pan S, Mueske CS, et al. Role for tissue factor pathway in murine model of vascular remodeling. *Circ Res.* 2001;89:71-76.
 34. Atsuchi N, Nishida T, Marutsuka K, et al. Combination of a brief irrigation with tissue factor pathway inhibitor (TFPI) and adenovirus-mediated local TFPI gene transfer additionally reduces neointima formation in balloon-injured rabbit carotid arteries. *Circulation.* 2001;103:570-575.
 35. Yin X, Yutani C, Ikeda Y, et al. Tissue factor pathway inhibitor gene delivery using HVJ-AVEliposome markedly reduces restenosis in atherosclerotic arteries. *Cardiovasc Res.* 2002;56:454-463.
 36. Channon KM, Qian HS, Youngblood SA, et al. Acute host-mediated endothelial injury after adenoviral gene transfer in normal rabbit arteries: impact on transgene expression and endothelial function. *Circ Res.* 1998;82:1253-1262.
 37. Ott I, Fischer EG, Miyagi Y, Mueller BM, Ruf W. A role for tissue factor in cell adhesion and migration mediated by interaction with actin-binding protein 280. *J Cell Biol.* 1998;140:1241-1253.
 38. Rogers C, Welt FG, Karnovsky MJ, Edelman ER. Monocyte recruitment and neointimal hyperplasia in rabbits: coupled inhibitory effects of heparin. *Arterioscler Thromb Vasc Biol.* 1996;16:1312-1318.
 39. Schecter AD, Rollins BJ, Zhang YJ, et al. Tissue factor is induced by monocyte chemoattractant protein-1 in human aortic smooth muscle and THP-1 cells. *J Biol Chem.* 1997;272:28568-28573.
 40. Rauch BH, Bretschneider E, Braun M, Schror K. Factor Xa releases matrix metalloproteinase-2 (MMP-2) from human vascular smooth muscle cells and stimulates the conversion of pro-MMP-2 to MMP-2: role of MMP-2 in factor Xa-induced DNA synthesis and matrix invasion. *Circ Res.* 2002;90:1122-1127.
 41. Selzman CH, Miller SA, Zimmerman MA, Gamboni-Robertson F, Harken AH, Banerjee A. Monocyte chemoattractant protein-1 directly induces human vascular smooth muscle proliferation. *Am J Physiol Heart Circ Physiol.* 2002;283:H1455-H1461.
 42. Herman MP, Sukhova GK, Kisiel W, et al. Tissue factor pathway inhibitor-2 is a novel inhibitor of matrix metalloproteinases with implications for atherosclerosis. *J Clin Invest.* 2001;107:1117-1126.
 43. Freter R, Alberta JA, Hwang GY, Wrentmore AL, Stiles CD. Platelet-derived growth factor induction of the immediate-early gene MCP-1 is mediated by NF-kB and a 90-kDa phosphoprotein co-activator. *J Biol Chem.* 1996;271:17417-17424.
 44. Friedman JM, Horwitz MS. Inhibition of tumor necrosis factor alpha-induced NF-kB activation by the adenovirus E3-10.4/14.5K complex. *J Virol.* 2002;76:5515-5521.
 45. Breuss JM, Cejna M, Bergmeister H, et al. Activation of nuclear factor-kB significantly contributes to lumen loss in a rabbit iliac artery balloon angioplasty model. *Circulation.* 2002;105:633-638.
 46. Siegbahn A, Johnell M, Rorsman C, Ezban M, Heldin CH, Ronnstrand L. Binding of factor VIIa to tissue factor on human fibroblasts leads to activation of phospholipase C and enhanced PDGF-BB-stimulated chemotaxis. *Blood.* 2000;96:3452-3458.
 47. Herbert J, Bono F, Herauld J, et al. Effector protease receptor 1 mediates the mitogenic activity of factor Xa for vascular smooth muscle cells in vitro and in vivo. *J Clin Invest.* 1998;101:993-1000.
 48. Blanc-Brude OP, Chambers RC, Leoni P, Dik WA, Laurent GJ. Factor Xa is a fibroblast mitogen via binding to effector-cell protease receptor-1 and autocrine release of PDGF. *Am J Physiol Cell Physiol.* 2001;281:C681-C689.
 49. Fishbein I, Waltenberger J, Banai S, et al. Local delivery of platelet-derived growth factor receptor-specific tyrophostin inhibits neointimal formation in rats. *Arterioscler Thromb Vasc Biol.* 2000;20:667-676.
 50. Mori E, Komori K, Yamaoka T, et al. Essential role of monocyte chemoattractant protein-1 in development of restenotic changes (neointimal hyperplasia and constrictive remodeling) after balloon angioplasty in hypercholesterolemic rabbits. *Circulation.* 2002;105:2905-2910.
 51. Poon M, Cohen J, Siddiqui Z, Fallon JT, Taubman MB. Trapidil inhibits monocyte chemoattractant protein-1 and macrophage accumulation after balloon injury in rabbits. *Lab Invest.* 1999;79:1369-1375.
 52. Ernoffsson M, Siegbahn A. Platelet-derived growth factor-BB and monocyte chemoattractant protein-1 induce human peripheral blood monocytes to express tissue factor. *Thromb Res.* 1996;83:307-320.
 53. Camerer E, Huang W, Coughlin SR. Tissue factor- and factor X-dependent activation of protease-activated receptor 2 by factor VIIa. *Proc Natl Acad Sci U S A.* 2000;97:5255-5260.
 54. Bretschneider E, Braun M, Fischer A, Wittpoth M, Glusa E, Schrör K. Factor Xa acts as a PDGF-independent mitogen in human vascular smooth muscle cells. *Thromb Haemost.* 2000;84:499-505.